Binomial stub loaded compact Vivaldi antenna for superwideband applications

Abhik Gorai[1] [iD] and Rowdra Ghatak[2]

[1]School of Electronics Engineering, KIIT Deemed University, Bhubaneswar, India and [2]ECE Dept, Microwave and Antenna Research Laboratory, National Institute of Technology Durgapur, West Bengal, India

Abstract

A compact antipodal Vivaldi antenna with superwideband characteristics is presented in this paper. For improved matching of input impedance at lower frequency region, techniques like binomial tapering of outer edges, binomial slit loaded outer edge, and protruded binomial tapered stub loading have been adopted. The antenna operates in a wide frequency range from 2 to 20 GHz. Experimental results show, stable radiation pattern with peak realized gain of more than 8 dBi, group delay within 1 ns, 164% fractional bandwidth, radiation efficiency of more than 90%, which are in good agreement with the simulated results. The compact size of the proposed antenna ($1.14\lambda_0 \times 1.21\lambda_0$) with wide frequency bandwidth and directional radiation characteristics make it suitable for through-wall radar and medical imaging applications.

CAMBRIDGE
UNIVERSITY PRESS

Introduction

The inherent property of wide bandwidth and directional radiation pattern has triggered the development of tapered slot antennas (TSAs) for medical imaging and through-wall imaging applications. TSA was first reported in the year 1979 by Gibson [1] which was also referred to as exponentially TSA or Vivaldi antenna. Thereafter, the development of Vivaldi antennas with different tapering profiles [2] was explored and reported. However, exponentially tapered slot Vivaldi antenna is mostly used owing to its least sidelobe levels as compared to linear TSA and constant width slot antennas [2]. Traditional TSAs have difficulty in broadband impedance matching of microstrip line and slot line resulting in the reduction of operating bandwidth. The difficulty in wideband impedance matching was vanquished by utilizing a tapered microstrip transition, through parallel strip lines, to symmetric double-sided slot line as proposed by Gazit [3]. It has directional radiation characteristics with maximum radiation in the end-fire direction. For invoking maximum radiation in the end-fire direction, the phases of the traveling wave current in either arm must be in the opposite phase. Thereafter the advantages of antipodal Vivaldi antenna (AVA) came to recognize in the wideband antenna design paradigm. Some earlier development of AVA included significant works reported in [4] and [5]. Attempt to reduce the size of the antenna and thereby exploring bandwidth enhancement techniques have been reported in [6, 7]. In [6], both circular loading and slot-loading techniques are adopted for improvement in impedance matching while in [7], exponential slot loading is done for improvement in impedance matching. One of the designs presents corrugation in the radiating arms for improving directivity and bandwidth [8]. An improvement in impedance bandwidth has been achieved by using a slot edge with exponential opening forming a palm tree-like structure [9]. A similar design has been reported in [10] where a side slotted Vivaldi antenna is reported to improve the impedance matching. In [11], a comparison of single petal structured Vivaldi antenna and dual petal structured Vivaldi antenna are compared. It is observed that a dual petal structured AVA offers more impedance bandwidth than a single petal structured AVA. In [12], it is shown that elliptical corrugations on the outer edge of AVA with optimal shaping of the inner edges of the antenna result in good impedance matching. Moreover, a patch compensated wideband Vivaldi antenna is reported in [13].

In this work, novel impedance matching techniques like binomial tapering of the outer edge, binomial slit loading, and protruded binomial stub loading are incorporated in the conventional antipodal Vivaldi antenna (CAVA) to increase the electrical length and thereby reducing the lower operating frequency. The proposed antenna has a fractional bandwidth of 164% and is compact compared to other related works [8–13]. The organization of the paper is as follows. The design methodology is described in the section "Antenna design methodology". Experimental results are compared with its predicted values and are presented in the section "Results and discussions" which is followed by a conclusion in the section "Conclusion".

Antenna design methodology

The diagrammatic representation of the proposed antenna is depicted in Fig. 1. The proposed AVA is binomially tapered, loaded with binomial slits, and binomial tapered stubs. Rigorous preliminary design alternatives and corresponding simulation data revealed that the binomial tapering is found to be more effective in impedance matching at lower frequencies, unlike conventional exponential tapering. However, for brevity, those have not been given here. All the simulations have been carried out using commercially available electromagnetic simulation software CST microwave studio™. The designed AVA has a compact size of 40.4 mm × 38 mm, etched on a low-cost FR4 substrate with permittivity of 4.4 and thickness 1.59 mm. The stages of development of the proposed antenna, described in this paper, are depicted in Fig. 2 and are detailed under the following subsections. The preliminary design analysis discloses that not all design tapering types can be applied brute force in achieving compact as well as wide impedance bandwidth. Some tapering may provide exceptionally suitable impedance bandwidth, but the overall size is large. So, in presenting the design in this work, the suitable alternative that satisfies impedance bandwidth, consistent radiation characteristics, as well as compact overall dimension was found to be offered by a Binomial tapering and a similar profile in the realization of the slit and stubs.

Design of the CAVA

The exponential inner tapering of CAVA is obtained from equation (1) [4].

$$y = \pm k_i \exp(a_i z), \ 0 \le z \le (L_s - L_f - g)$$

$$0 \le z \le (L_s - L_f - g). \tag{1}$$

In (1), a is the coefficient that relates the slot widening and k_i is half of the total slot width at the feed interface of the antenna. Similarly, the outer edge of CAVA is obtained by using equation (2) [4].

$$y = \pm k_0 \exp(a_0 z^b), \ 0 \le z \le l_b, \tag{2}$$

where k_0 is the cumulative value of one of the conductors at the feed and k_i. The coefficient b relates to the shape of the outer edge taper. The maximum separation between the arms of CAVA is set at $\lambda_g/2$ at the lowest frequency. The optimized values of k_i, a_i, k_0, a_0, and b are 0.13, 0.15, 1.6, 0.01, and 2 respectively. As depicted in Fig. 2, the bandwidth obtained by CAVA ranges from 3 to 20 GHz. For the CAVA to have wide operational bandwidth, the phases of the traveling wave currents on each arm have to be 180^0 apart. However, the limiting factors of the bandwidth are tapering of the slot radiator, the width of the feed line, and transition from the feed line to the radiator.

Effect of binomial tapering of the outer edge

Binomial tapering [14] of the outer edge of CAVA is done according to equation (3).

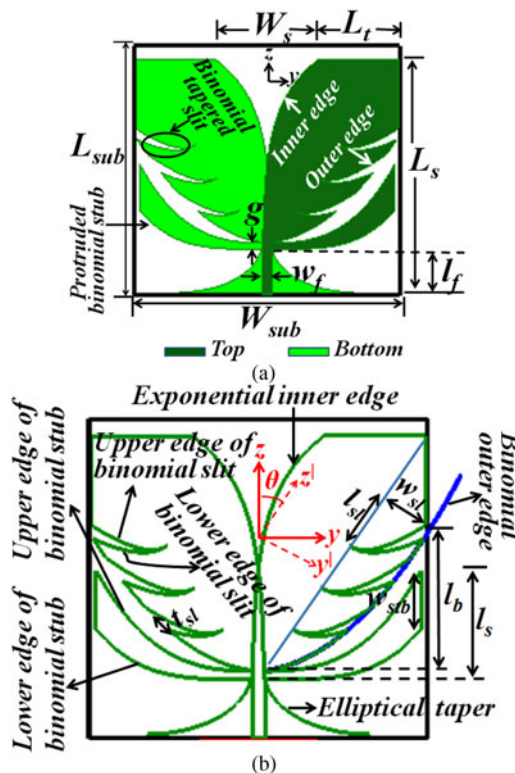$$z = l_b \left(\frac{y}{\frac{W_s}{2} + L_t} \right)^N, \ 0 \le y \le \frac{W_{sub}}{2}. \tag{3}$$

Fig. 1. (a) Layout of the proposed antenna, (b) details of various tapering profiles. $L_{sub} = 38$, $W_{sub} = 40.4$, $W_s = 15.8$, $L_t = 12.08$, $L_s = 36$, $l_f = 7$, $w_f = 1.47$, $g = 1$, $t_{sl} = 3.47$, $w_{stb} = 7$, $l_b = 17.22$, $l_s = 13$, $w_{sl} = 6.8$, $l_{sl} = 7$ (in mm).
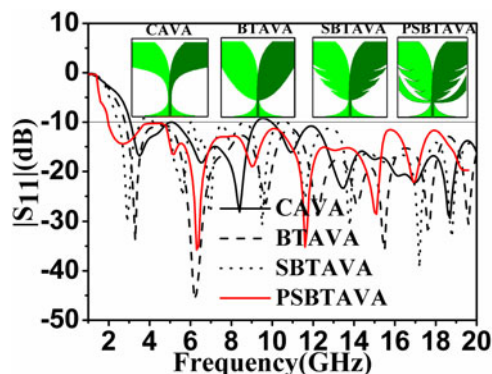

Fig. 2. Evolution of the proposed AVA.

In CAVA, the flare length in terms of wavelength is much shorter in lower frequencies, resulting in less efficient radiation of current on the flare. Binomial tapering of outer edge results in an increase in electrical length along the outer edge, which shifts the first resonant frequency in the lower frequency region. As depicted in Fig. 2, the bandwidth obtained by binomial tapered antipodal Vivaldi antenna (BTAVA) ranges from 2.8 to 20 GHz. A parametric study with different values of the order of binomial function N was carried out and is depicted in Fig. 3. It is revealed that, when $N = 1$, there is an impedance mismatch around 9 and 11 GHz. Moreover, binomial tapering in the order of $N = 3$ also results in impedance mismatch around 5 GHz. The best result of $|S_{11}|$ characteristics is obtained when $N = 2$.
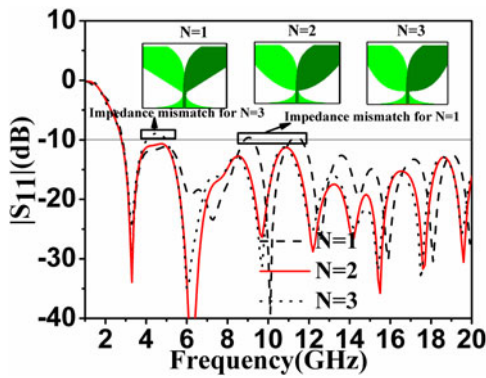
Fig. 3. Effect of variation of $|S_{11}|$ characteristics for different values of N.
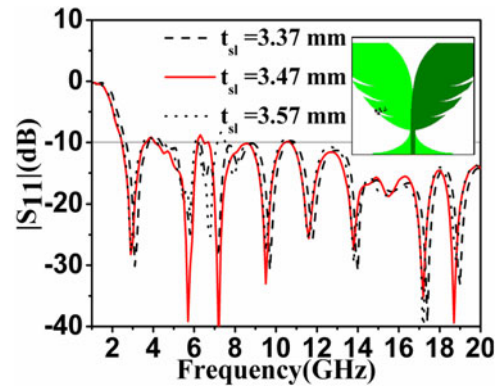

Fig. 4. Effect of variation of $|S_{11}|$ characteristics for different values of $N^|$.

Fig. 5. Effect of variation of $|S_{11}|$ characteristics for different values of l_{sl}.
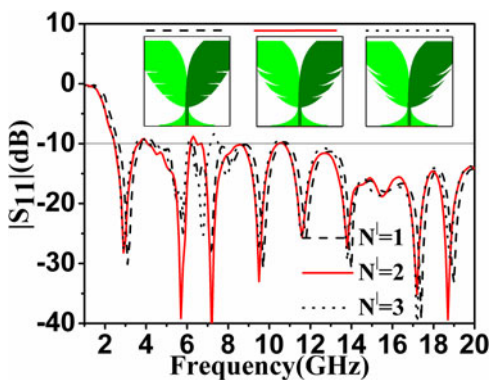

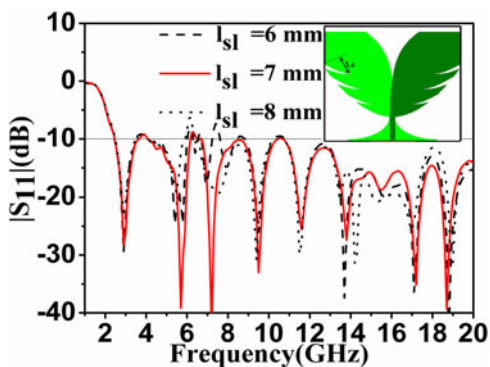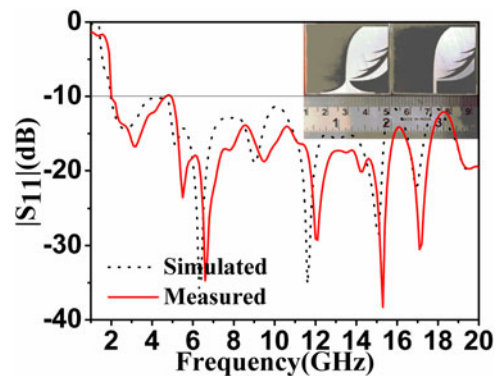Fig. 6. Effect of variation of $|S_{11}|$ characteristics for different values of t_{sl}.

Fig. 7. Comparison of simulated and measured $|S_{11}|$ characteristics.
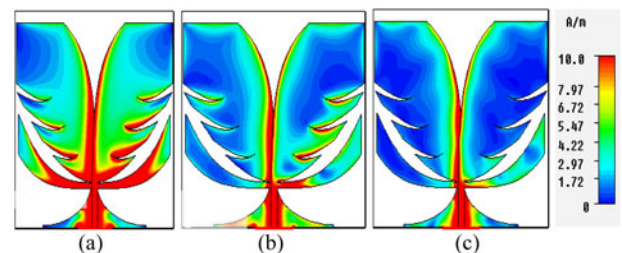
Fig. 8. Current distribution at (a) 2.5 GHz, (b) 10 GHz, and (c) 18 GHz.

$$z^| = (l_{sl} - t_{sl}) \left(\frac{y^|}{w_{sl}} \right)^{N^|}, \ 0 \le y^| \le w_{sl}, \tag{5}$$

where $z^| = z\cos\theta$ and $y^| = y\cos\theta$, and θ is defined by (6).

$$\theta = \tan^{-1} \left(\frac{L_s}{\frac{W_s}{2} + L_t} \right). \tag{6}$$

The other slits are constructed similarly and are separated by l_{sl} and the value of $N^|$ is taken to be 2. The effect of variation of the order of binomial function $N^|$ is shown in Fig. 4. The observation reveals that when $N^|$ increases from 1 to 2, the first resonant frequency shifts to lower frequency region, thereby increasing the impedance matching at lower frequencies. However, no

Effect of binomial slits in the outer edge

Further improvement in input impedance matching in low-frequency region can be accomplished by etching binomial slits along the outer edges (Fig. 1). Binomial slits are designed according to the design principle proposed in [14]. The slit near to the feed, in either conductor, is created by employing (4) and (5).

$$z^| = l_{sl} \left(\frac{y^|}{w_{sl}} \right)^{N^|}, \ 0 \le y^| \le w_{sl}, \tag{4}$$

Fig. 9. Simulated and proposed radiation pattern of the proposed AVA in *xz* plane and *yz* plane at (a) 2 GHz, (b) 7 GHz, (c) 12 GHz, and (d) 20 GHz.
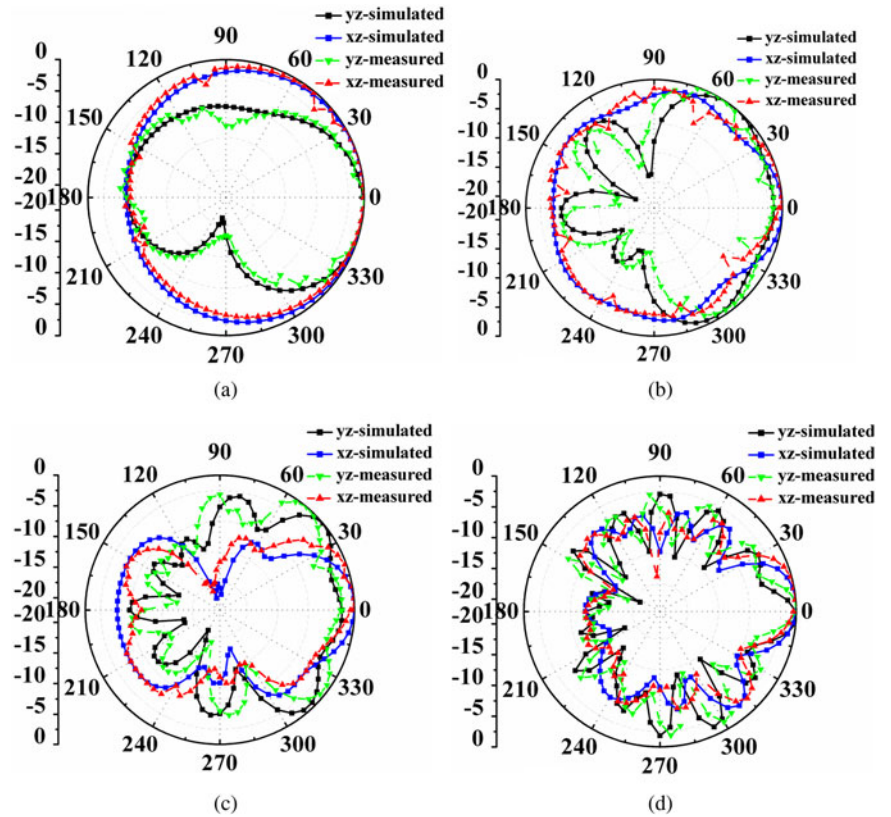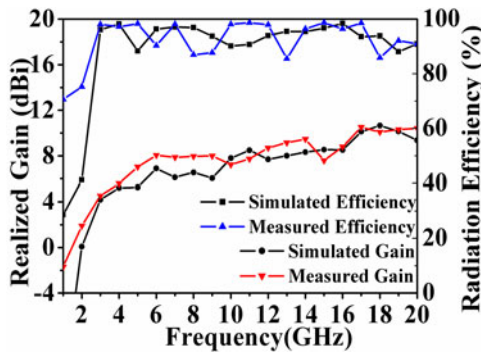

Fig. 10. Simulated and measured gain and efficiency of the proposed antenna.
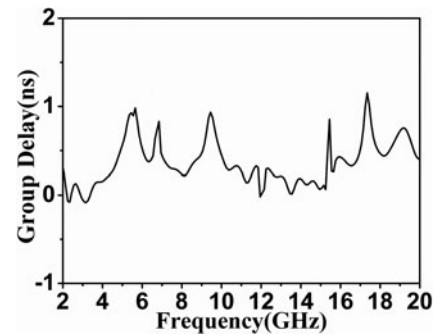

Fig. 11. Group delay profile of the proposed AVA.

significant change in $|S_{11}|$ characteristics is observed on further increase in N^l.

Moreover, the impedance matching around 6–8 GHz is affected by the variation in length l_{sl} as shown in Fig. 5. It is observed that the best impedance matching is obtained when the value l_{sl} is 7 mm.

The parametric study of t_{sl} is done and is reported in Fig. 6. It is observed that, increase in t_{sl} shifts the first resonant frequency in the lower frequency region. However, the best result is achieved when the value of t_{sl} is 3.47 mm. Further increase in t_{sl} does not have a significant effect on $|S_{11}|$ characteristics.

Effect of binomial stubs in the outer edge

A binomial tapered stub is appended near to the feed to introduce some additional modes and thereby further increasing the input

Table 1. Fidelity factors of the proposed AVA in two principle planes

xz plane		yz plane	
θ(°)	PFF	θ(°)	PFF
0	0.9975	0	0.9904
30	0.9543	30	0.9615
60	0.9012	60	0.8876
90	0.5652	90	0.5012

impedance matching in lower frequencies. As shown in Fig. 2, the impedance bandwidth of the protruded stub BTAVA exhibits an impedance bandwidth that ranges from 2 to 20 GHz. The design of the protruded stub is governed by the following

Table 2. Comparison of the existing literature with the proposed antenna

	Dielectric constant	Physical size $(l \times w)$	Percentage bandwidth (%)	Peak gain	Efficiency
[8]	4.4	45 × 40	122	12 dBi	89%
[9]	6.15	59.81 × 36.30	65.06	8 dBi	–
[10]	2.33	45 × 37	80	6.8 dBi	88%
[11]	4.3	60 × 60	146.82	5 dBi	–
[12]	3.38	121 × 82	147.82	14.7 dBi	–
[13]	4.33	110 × 80	29	–	–
Our work	4.4	38 × 40.4	164	8 dBi	>90%

equations.

$$z = l_s \left(\frac{y}{\frac{W_s}{2} + L_t} \right)^{N^{\|}}, \ 0 \le y \le \frac{W_s}{2} + L_t, \qquad (7)$$

$$z = (l_s - w_{stb}) \left(\frac{y}{\frac{W_s}{2} + L_t} \right)^{N^{\|\|}} - g, \ 0 \le y \le \frac{W_s}{2} + L_t. \qquad (8)$$

The values of the orders $N^{\|}$ and $N^{\|\|}$ of binomial functions are 3 and 4, respectively.

Results and discussions

The fabricated prototype of the proposed antenna is shown in the inset of Fig. 7. The affirmation of the simulated S-parameter results of the proposed antenna is done using Rhode and Schwarz ZVA 40 VNA and is portrayed in Fig. 7. A small discrepancy between simulated and measured $|S_{11}|$ dB characteristics is due to inaccuracy in the soldering of the SMA connectors. The measured impedance bandwidth of the proposed antenna ranges from 2 to 20 GHz. The current distribution plot of the proposed Vivaldi antenna at frequencies 2.5, 10, and 18 GHz are shown in Fig. 8. It is observed that the current density is significant along the edges of the binomial slots and in the binomial tapered slots at lower frequencies, which indicates an effective enhancement of the current path resulting in an increase in lower-end bandwidth.

The simulated and measured radiation patterns at different frequencies are shown in Fig. 9. End fire radiation properties are observed throughout the operational bandwidth. Higher-order modes are generated at higher frequencies resulting in some ripples in the radiation patterns which is observed in Fig. 9. Peak realized gain of the proposed antenna is more than 8 dBi as depicted in Fig. 10. Moreover, the simulated and measured radiation efficiency of the proposed antenna is also depicted in Fig. 10. It is observed that the radiation efficiency is more than 90% for the proposed AVA.

Phase linearity within the operational bandwidth is an important aspect of wideband antenna design. For this, the maximum acceptable group delay must be within $D_t = (1/2f_s)$ [15]. It is observed from Fig. 11 that the group delay response is almost flat, which indicates distortion-less transmission. Moreover, the

pulse fidelity factor is also an important performance metric of the antenna in the time domain. The fidelity factor shows the amount of similarity between the transmitted and received pulses. The fidelity factor is determined by utilizing equation (9).

$$\rho = \max \left\{ \frac{\int s_t(t) s_r(t - \tau) dt}{\sqrt{s_t^2(t) \sqrt{s_r^2(t)}}} \right\}, \qquad (9)$$

where $s_t(t)$ and $s_r(t)$ are input signal and received signal, respectively. The transmitting antenna and receiving antenna are kept at a far-field distance at the lower frequency of the operational bandwidth [16]. Fidelity factors for different orientations of transmit-receive antenna systems in xz plane and yz plane are obtained and tabulated in Table 1. It is revealed that as the signals approach orthogonality, the fidelity factor decreases.

A comparison of the proposed Vivaldi antenna with the previously reported Vivaldi antennas in [8–13] is tabulated in Table 2. It is revealed, that the proposed antenna is compact and has the highest percentage bandwidth of 164%. Moreover, the proposed Vivaldi antenna has an efficiency of 90%.

Conclusion

In this work, binomial tapering of outer edges of antipodal Vivaldi antenna, loaded with binomial slits and binomial tapered stubs have been found suitable for improving impedance matching in the lower frequency region and thereby achieves super wideband characteristics. It has been observed that the antenna exhibits a percentage bandwidth of 164% with satisfactory end-fire radiation characteristics. The conventional trend of increase in directivity with frequency is observed for the proposed antenna. The flat group delay profile of the antenna confirms the non-dispersive nature of the proposed antenna and thereby prevents the generation of time-varying non-linearity translating to higher-order resonances. Moreover, the antenna also shows a high peak realized gain of more than 8 dBi. Assembling all these properties of the designed antenna, make it suitable for through-wall imaging and medical imaging applications.

References

1. **Gibson PJ** (1979) The Vivaldi aerial, in *Proc. 9th Euro. Microw. Conf.*, Brighton, U.K., Oct. 1979, pp. 101–105.
2. **Yngresson KS, Schaubert DH, Korzeniowski TL, Kollberg EL, Thungren T and Johansson JF** (1985) End fire tapered slot antennas

on dielectric substrates. *IEEE Transactions on Antennas and Propagation* **33**, 1392–1400.

3. **Gazit E** (1988) Improved design of the Vivaldi antenna. *IEE Proceedings H (Microwaves, Antennas and Propagation)* **135**, 89–92.

4. **Greenberg MC, Virga KL and Hammod CL** (2003) Performance characteristics of the dual exponentially tapered slot antenna (DETSA) for wireless communication application. *IEEE Transaction on Vehicular Technology* **52**, 305–312.

5. **Siddiqui JY, Antar YMM, Freundorfer AP, Smith EC, Morin GA and Thayaparan T** (2011) Design of an ultrawideband antipodal tapered slot antenna using elliptical strip conductors. *IEEE Antennas and Wireless Propagation Letters* **10**, 251–254.

6. **Bai J, Shi S and Prather DW** (2011) Modified compact antipodal Vivaldi antenna for 4–50 GHz UWB application. *IEEE Transactions on Microwave Theory and Techniques* **59**, 1051–1057.

7. **Fei P, Jiao Y-C, Hu W and Zhang F-S** (2011) A miniaturized antipodal Vivaldi antenna with improved radiation characteristics,". *IEEE Antennas and Wireless Propagation Letters* **10**, 127–130.

8. **Pandey GK and Meshram MK** (2015) A printed high gain Vivaldi antenna design using tapered corrugation and grating elements. *International Journal of RF and Microwave Computer-Aided Engineering* **25**, 610–618.

9. **De Oliveira AM** (2015) A palm tree antipodal Vivaldi antenna with exponential slot edge for improved radiation pattern. *IEEE Antennas and Wireless Propagation Letters* **15**, 1334–1337.

10. **Mahmud MZ, Islam MT, Samsuzzaman M, Kibria S and Misran N** (2017) Design and parametric investigation of directional antenna for microwave imaging application. *IET Microwaves, Antennas and Propagation* **11**, 770–778.

11. **Natarajan R, George JV, Kanagabasai M, Lawrance L, Moorthy B, Rajendran DB and Alsath MGN** (2016) Modified antipodal Vivaldi antenna for ultrawideband communications. *IET Microwaves, Antennas and Propagation* **10**, 401–405.

12. **Malakooti S-A, Moosazadeh M, Ranasinghe DC and Fumeaux C** (2017) Antipodal Vivaldi antenna for sum and difference radiation patterns with reduced grating lobes. *IEEE Antennas and Wireless Propagation Letters* **16**, 3139–3142.

13. **Yadav RP, Kumar V and Rajveer D** (2018) Design and development of patch compensated wideband Vivaldi antenna. *International Journal of Microwave and Wireless Technologies* **10**, 1081–1087.

14. **Ling C-W, Lo W-H, Yan R-H and Chung S-J** (2007) Planar binomial curved monopole antennas for ultrawideband communication. *IEEE Transactions on Antennas and Propagation* **55**, 2622–2624.

15. **Perez-Martinez F, Burgos-Garcia M and Asensio-Lopez A** (2001) Group delay effects on the performance of wideband CW-LFM radars. *IEE Proceedings-Radur, Sonar and Navigation* **148**, 95–100.

16. **Yang Y-Y, Chu Q-X and Zheng Z-A** (2009) Time domain characteristics of band notched ultrawideband antenna. *IEEE Transactions on Antennas and Propagation* **57**, 3426–3430.

Abhik Gorai received his M.Tech from National Institute of Technology, Durgapur. He started his career as an engineer in Huawei Telecommunication and thereafter, he served in Alkatel Lucent. He is presently an Assistant Professor in the School of Electronics engineering of KIIT Deemed University. His interest lies in fractal antennas, metamaterials, MIMO Antennas, and SIW Antennas. He is a reviewer of IEEE, IET, IETE, and Elsevier journals.

Rowdra Ghatak received his M.Tech (Microwave Engineering) from The University of Burdwan and Ph.D. (Engg) from Jadavpur University. He initiated his career in microwave engineering as a trainee at CEERI Pilani in fabrication and testing of S-band magnetrons. Thereafter he served at the National Institute of Science and Technology Berhampur, Odisha and at the University of Burdwan. He is presently a Professor in Electronics and Communication Engineering Department of National Institute of Technology Durgapur. He is a recipient of the URSI Young Scientist Award in 2005. He received support under DST Young Scientist scheme for development of UWB antennas for imaging RADAR. He has more than 250 publications in various National/International journals and conferences. His research interest lies in the areas of the fractal antenna, metamaterials, application of evolutionary algorithms to electromagnetic optimization problems, RFID, computational electromagnetic and microwave passive and active circuit design. He is a reviewer of IEEE, IET, Elsevier, John Wiley, and Springer journals. He has organized workshops in the capacity of workshop chair/convener on Microwave Circuits and Antenna and has been a member of technical program committee membership of numerous IEEE conferences in the Asia Pacific region. He was a student paper contest co-Chair in the IEEE AEMC 2013 and Technical program co-chair at IEEE MicroCom 2016 and conducted numerous technical lectures.